# Development of a unit-based industrial emission inventory in the Beijing-Tianjin-Hebei region and resulting improvement in air quality modeling

Haotian Zheng[a, 1], Siyi Cai[a, 1], Shuxiao Wang[a], Bin Zhao[b], Xing Chang[a], Jiming Hao[a]

[a]School of Environment and State Key Joint Laboratory of Environment Simulation and Pollution Control, Tsinghua University, Beijing 100084, China
[b]Joint Institute for Regional Earth System Science and Engineering and Department of Atmospheric and Oceanic Sciences, University of California, Los Angeles, CA 90095, USA

*Correspondence to*: S. Wang (shxwang@tsinghua.edu.cn) and B. Zhao (zhaob1206@ucla.edu)

[1] These authors contributed equally to this study.

**Abstract.**

The Beijing-Tianjin-Hebei (BTH) region is a metropolitan area with the most severe fine particle ($PM_{2.5}$) pollution in China. Accurate emission inventory plays an important role in air pollution control policy making. In this study, we develop a unit-based emission inventory for industrial sectors in the BTH region, including power plants, industrial boilers, and steel, non-ferrous metal, coking, cement, glass, brick, lime, ceramics, refinery, and chemical industries, based on detailed information for each enterprise, such as location, annual production, production technology/process and air pollution control facilities. In the BTH region, the emissions of sulfur dioxide ($SO_2$), nitrogen oxide ($NO_x$), particulate matter with diameter less than 10 μm ($PM_{10}$), $PM_{2.5}$, black carbon (BC), organic carbon (OC), and non-methane volatile organic compounds (NMVOCs) from industrial sectors are 869 kt, 1164 kt, 910 kt, 622 kt, 71 kt, 63 kt and 1390 kt in 2014, respectively, accounting for 61%, 55%, 62%, 56%, 58%, 22% and 36%, respectively, of the total emissions. Compared with the traditional proxy-based emission inventory, much less emissions in the high-resolution unit-based inventory are allocated to the urban center because of the accurate positioning of industrial enterprises. We apply the Community Multi-scale Air Quality (CMAQ) model simulation to evaluate the unit-based inventory. The simulation results show that the unit-based emission inventory gives better performance of both $PM_{2.5}$ and gaseous pollutants than the proxy-based emission

inventory. The normalized mean biases (NMBs) are 81%, 21%, 1% and -7% for concentrations of $SO_2$, $NO_2$, ozone and $PM_{2.5}$, respectively, with the unit-based inventory, in contrast to 124%, 39%, -8% and 9% with the proxy-based inventory. Furthermore, the concentration gradients of $PM_{2.5}$, which are defined as the ratio of urban concentration to suburban concentration, are 1.6, 2.1 and 1.5 in January and 1.3, 1.5

5  and 1.3 in July, for simulations with the unit-based inventory, simulations with the proxy-based inventory, and observations, respectively, in Beijing. For ozone, the corresponding gradients are 0.7, 0.5 and 0.9 in January and 0.9, 0.8 and 1.1 in July, implying that the unit-based emission inventory better reproduces the distributions of pollutant emissions between the urban and suburban areas.

10  **1 Introduction**

The Beijing-Tianjin-Hebei (BTH) region is the political, economic and cultural center of China. According to China National Environmental Monitoring Centre (data source: http://106.37.208.233:20035/), in 2017, the annual average concentration of $PM_{2.5}$ in Beijing, Tianjin and Hebei are 65.6, 63.8 and 57.1 $\mu g/m^3$, ranking second, third and sixth among all provinces. The severe

15  $PM_{2.5}$ pollution in the BTH region is largely attributed to the substantial emissions of air pollutants (Zhao et al., 2017a). An accurate emission inventory, in terms of both emission rates and spatial distribution, is imperative for an adequate understanding of the sources and formation mechanism of the serious air pollution.

The spatial distribution is one of the most uncertain component of emission inventories considering the

20  diverse source categories and complex emission characteristics. The traditional method of spatial allocation is to distribute the emissions by administrative region into grids based on spatial proxies such as population, gross domestic product (GDP), road map, land use data and nighttime lights (Geng et al., 2017;Oda and Maksyutov, 2011;Streets et al., 2003). The results may deviate significantly from the actual spatial distributions of many sources (Zhou and Gurney, 2011), especially the power and industrial

25  sources, which contribute over 50% of the total $PM_{2.5}$ emissions in China (Zhao et al., 2013a). Due to the

stricter air quality regulation and higher land price in urban area, people tend to build factories in suburban area where the population density and GDP are lower. Zheng et al. (2017) studied the influence of the resolution of gridded emission inventory and found that there were large biases when the inventory was distributed to very fine resolution following the traditional proxy-based allocation method. The emission

5 inventory could be significantly improved with detailed information of point sources such as power plants, steel plants, cement plants, etc. The high spatial resolution of the inventory may subsequently improve the air quality modeling results and enable a better source apportionment of air pollution (Zhao et al., 2017c).

A couple of studies have developed the emission inventory in the BTH region (Li et al., 2017;Lim et al.,

10 2005;Wang et al., 2014), and some others have provided emission estimates for this region as part of national or larger-scale emission inventories (Ohara et al., 2007;Stohl et al., 2015). However, only limited studies estimated the emissions by individual point sources (i.e., unit-based emission inventory). Zhao et al. (2008) and Chen et al. (2014) established unit-based emission inventories of coal-fired power plants in China. Wang et al. (2016) developed an emission inventory of steel industry from 1978 to 2011. Lei et

15 al. (2011) established an emission inventory of cement industry in China from 1990 to 2020. Qi et al. (2017) established an emission inventory in BTH region with power and major industrial sources treated as point sources. These studies usually focused on one or several major industries, and did not cover all industrial sectors in the BTH region. Moreover, these previous studies seldom validated the unit-based emission inventory or evaluated the improvement it brings to air quality simulation.

20 In this study, we developed a unit-based emission inventory of industrial sectors for the Beijing-Tianjin-Hebei region. A three-domain nested simulation by WRF-CMAQ model was applied to evaluate the emission inventory. In order to study the influence of the point sources, we compared the simulation results of this emission inventory with the those of a traditional proxy-based emission inventory.

## 2 Materials and methods

### 2.1 High-resolution emission inventory for Beijing-Tianjin-Hebei region

A unit-based method is applied to quantify the emissions from industrial sectors such as power plant, industrial boiler, iron and steel production, non-ferrous metal smelter, coking, cement, glass, brick, lime,

5  ceramics, refinery, and chemical industries in 2014. The pollutant emissions from each industrial enterprise are calculated from activity level (energy consumption for power plants and industrial boilers, and product yield for other sectors), emission factor, and removal efficiency of control technology, as shown in the following equation:

$$E_i = \sum_j E_{i,j} = \sum_j \left( \sum_m A_{j,m} \times EF_{i,m} \times \left(1 - \eta_{i,m,n}\right) \right) \quad (1)$$

10  where E is emissions, A is activity level, EF is uncontrolled emission factor, and η is removal efficiency of control technology. Additionally, i, j, m, and n are parameters that represent the type of pollutants, industrial enterprise, production process and control technology. The EFs are calculated according to the sulfur and ash contents of fuels (e.g. coal) used in each enterprise, or obtained from our previous study (Zhao et al., 2013b).

15  For industrial enterprises with multiple stages of production, such as cement plants, the equation is as follows:

$$E_{i,j} = \sum_m \left( AK_{j,m} \times EF_{i,m} \times \left(1 - \eta_{i,m,n}\right) \right) + \left( AC_j \times ef_i \times \left(1 - \eta_{i,k}\right) \right) \quad (2)$$

where $E_{i,j}$ is emissions of pollutant **i** from industrial enterprise **j**, $AK_{j,m}$ is the amount of clinker produced by the clinker burning process **m** of the enterprise **j**, $EF_{i,m}$ is uncontrolled emission factor for pollutant **i**

20  from the clinker burning process **m**, $\eta_{i,m,n}$ is removal efficiency of control technology **n**, $AC_j$ is the amount of cement produced by enterprise **j**, $ef_i$ is uncontrolled emission factors from the clinker processing stage ($ef_i$=0 if **i** is not particulate matter), $\eta_{i,k}$ is removal efficiency of control technology **k**. For all power and industrial sources except industrial boilers, we collect their detailed information, including latitude/longitude, annual product, production technology/process, and pollution control

25  facilities from the related industrial associations (i.e. China Electricity Council, China Steel Yearbook,

China Cement Association), statistical yearbooks (i.e. Environmental Statistics), and large-scale survey data from government. These emission sources include 242 power plants, 333 iron and steel plants, 639 cement plants, 151 nonferrous metal smelters, 211 lime plants, 1222 brick and tile plants, 37 ceramic plants, 42 glass plants, 106 coking plants, 21 refinery plants, and 328 chemical plants. For industrial

5    boilers, we obtained the location and fuel use amount of over 8 thousand industrial boilers in Beijing, Tianjin, and Hebei from Xue et al. (2016), Tianjin Environmental Protection Bureau, and Hebei Environmental Protection Bureau.

The emission inventory for other sources, including residential sources, transportation, solvent use, and open burning, is developed based on the "emission factor method" following our previous work (Fu et al.,

10    2013;Wang et al., 2014;Zhao et al., 2013b). The method is the same as **Eq (1)** except that the emissions are calculated for individual prefecture-level city rather than individual enterprise. The activity data and technology distribution for each sector are derived based on the Statistics Yearbook (Beijing Municipal Bureau of Statistics, 2015;Hebei Municipal Bureau of Statistics, 2015;National Bureau of Statistics (NBS), 2015i, j, a, b, h, c, d, e, f, g;Tianjin Municipal Bureau of Statistics, 2015), a wide variety of Chinese technology reports (China

15    Electricity Council, 2015;National Bureau of Statistics (NBS), 2012), and an energy demand modeling approach. **Fig.S1** shows energy consumption in the BTH region in 2014. The emission factors are also obtained from Zhao et al. (2013b). The speciation of $PM_{2.5}$ is from Fu et al. (2013). The speciation of NMVOCs is updated by Wu et al. (2017) The penetrations of removal technologies are obtained from the evolution of emission standards and a variety of technical reports (Chinese State Council, 2013).

## 20    2.2 Air quality model configuration

In this work, we use CMAQ version 5.0.2 to simulate the concentration of pollutants. A three-domain nested simulation is established as shown in **Fig. 1** (left). The first domain covers almost entire area of China, Korea, Japan, and parts of India and Southeast Asia with a horizontal grid resolution of 36 km × 36 km. The second domain covers eastern China with a resolution of 12 km × 12 km. The third domain

25    with a horizontal resolution of 4 km × 4 km focuses on the Beijing-Tianjin-Hebei region. The observational sites in Beijing-Tianjin-Hebei region are marked in **Fig. 1** (right). All of the grids are

divided to 14 layers vertically from surface to an altitude of about 19 km above the ground and the thickness of the first layer is about 40 m.

In order to minimize the influence of initial condition, we choose 5 days of spin-up period. The Carbon Bond 05 (CB05) and AERO6 are chosen as the gas-phase and aerosol chemical mechanisms, respectively.

5 The simulation periods are January and July of 2014, representing winter and summer, respectively.

We use the Weather Research and Forecasting (WRF) model version 3.7.1 to simulate the meteorological fields. The physics options for the WRF simulation are the Kain-Fritsch cumulus scheme, the Morrison double-moment scheme for cloud microphysics, the Pleim-Xiu land surface model, Pleim-Xiu surface layer scheme, ACM2 (Pleim) boundary layer parameterization, and Rapid Radiative Transfer Model for

10 GCMs radiation scheme. Other configurations are the same as Zhao et al. (2013b). The Meteorology Chemistry Interface Processor (MCIP) version 4.1 is applied to process the meteorological data into a format required by CMAQ. The simulated wind speed, wind direction, temperature and humidity agree well with the observation data from the National Climate Data Center (NCDC), as detailed in the Supplementary Information.

15 In order to evaluate the high-resolution emission inventory with unit-based industrial sources, we developed a traditional proxy-based emission inventory with the same amount of emissions and compare the simulation results of these two emission inventories. In the proxy-based emission inventory, all sectors are allocated as area sources using spatial proxies such as population, GDP, road map and land use data.

## 3 Results and discussion

20 ### 3.1 Air pollutant emissions in Beijing-Tianjin-Hebei region

In the BTH region, the emissions of sulfur dioxide ($SO_2$), nitrogen oxide ($NO_x$), $PM_{10}$, $PM_{2.5}$, black carbon (BC), organic carbon (OC), non-methane volatile organic compounds (NMVOCs) and ammonia ($NH_3$) are 1417 kt, 2100 kt, 1479 kt, 1106 kt, 213 kt, 289 kt, 2381 kt, and 712 kt in 2014, respectively. **Fig. 2** shows the sectoral emissions for major pollutants in the BTH region by city. **Fig.S2** shows the NMVOCs

25 speciation by sector. The emission estimates are compared with previous studies in **Fig.S3**.

Power plants account for 13%, 16%, and 4% of the total $SO_2$, $NO_x$, and $PM_{2.5}$ emissions, respectively, and the contributions to NMVOC and $NH_3$ emissions are negligible (< 1%). For $SO_2$ and $NO_x$, power plant is an important emission sources in the BTH region, especially in Tianjin, Shijiazhuang, Tangshan, and Handan.

5   The emissions from industrial boiler account for 27%, 19%, 8%, 1%, and < 1% of the total $SO_2$, $NO_x$, $PM_{2.5}$, NMVOCs, and $NH_3$ emissions, respectively. As shown in **Fig. 2**, there are many industrial boilers in the BTH region. Industrial boiler is one of the most important emission sources for $SO_2$ and $NO_x$.

The emissions from cement contribute 6%, 9%, and 10% of the total $SO_2$, $NO_x$, and $PM_{2.5}$ emissions, respectively, and the contributions to NMVOC and $NH_3$ emissions are negligible (< 1%). Most of cement
10   plants are located in South and East of Hebei.

The emissions from steel represent 8%, 3%, and 22% of the total $SO_2$, $NO_x$, and $PM_{2.5}$ emissions, respectively, and the contributions to NMVOC and $NH_3$ emissions are negligible (< 1%). Tangshan has the largest number of steel plants in the BTH region, steel accounts for over half of $PM_{2.5}$ emissions in Tangshan.

15   Besides the aforementioned sectors, 8%, 8%, 13%, 36%, and < 1% of the total $SO_2$, $NO_x$, $PM_{2.5}$, NMVOCs, and $NH_3$ emissions come from other industrial processes (chemistry, coking, nonferrous metal, brick, ceramics, lime, glass, refinery), respectively. Industrial process is the most important emission source for NMVOCs, accounting for nearly half of the emissions in Tianjin and Shijiazhuang.

In total, in the BTH region, industrial sectors (power plant, industrial boiler, cement, steel, and other
20   industrial process) contribute 61%, 55%, 62%, 56%, 58%, 22%, 36% and 0% of the total $SO_2$, $NO_x$, $PM_{10}$, $PM_{2.5}$, BC, OC, NMVOCs, and $NH_3$ emissions in 2014. **Fig. 3** shows the locations and emissions of power and industrial sources.

Considering the large contribution of industrial sources to total emissions, the application of unit-based method results in remarkable changes in the spatial distribution of air pollutant emissions. The emission
25   rates of $PM_{2.5}$, $NO_x$ and $SO_2$ of the proxy-based and unit-based inventories and their differences are shown in **Fig. 4**. In the unit-based emission inventory, the emission is lower than that in the proxy-based emission

inventory in the urban centers of BTH region. Instead, a large amount of the emission is concentrated in certain points in suburban areas, where large plants are located.

## 3.2 Evaluation of the unit-based emission inventory

In order to study the accuracy of the unit-based inventory, the simulation results of $SO_2$, $NO_2$, ozone and
5   $PM_{2.5}$ with the unit-based inventory are compared with the observational data from China National Environmental Monitoring Centre. The results with the proxy-based inventory are also shown for reference purpose. The observations are available for eighty sites located in 13 cities in the BTH region, including 70 sites in urban area and 10 sites in suburban area. The analysis of the results is shown in **Table 1**. We use normalized mean bias (NMB), normalized mean error (NME), mean fractional bias
10   (MFB) and mean fractional error (MFE) (EPA, 2007) to quantitatively evaluate the model performance. $SO_2$ and $NO_2$ are precursors of $PM_{2.5}$, so we first compare the simulation results of gaseous pollutants with observations. For $NO_2$, the results with proxy-based inventory overestimates the observations by 22% while results with unit-based inventory overestimates by 9% in January. Similarly, in July, the simulated $NO_2$ concentrations show overestimation in simulations with both inventories but the overestimation is
15   less with unit-based inventory. The simulation results of $SO_2$ is similar to those of $NO_2$. However, the overestimation is higher with both inventories and the differences between the concentrations with two inventories are larger.

For ozone, the simulation results in January with proxy-based inventory underestimate the observations by 21% while the results with unit-based inventory underestimate by only 5%. The simulation results in
20   July follows the same trend. The reason for the changes in ozone concentrations will be discussed later. The simulated $PM_{2.5}$ concentrations with unit-based inventory are lower than that with proxy-based inventory in both winter and summer. In January, the simulated $PM_{2.5}$ concentrations with proxy-based inventory overestimates the observed values by 25% while the overestimation is 7% with unit-based inventory. In July, the simulated $PM_{2.5}$ concentrations with both inventories are 17% and 30% lower than
25   the observations, respectively. An overall underestimation is as expected because the default CMAQ model underestimates the concentrations of secondary organic aerosol (Zhao et al., 2016) significantly

and the fugitive dust emission is not included in the emission inventory. According to Boylan and Russell (2006), the simulation results of PM is acceptable when Mean Fractional Bias (MFB) is less than or equal to ±60% and Mean Fractional Bias (MFE) is less than 75% and a model performance goal is met when MFB is less than ±30% and MFE is less than 50%. The statistical indices of the simulation results of

5 $PM_{2.5}$ with both inventories and both months are within the performance goal value, which means that the simulation results are relatively accurate.

**Fig. 5** further shows the spatial distribution of $SO_2$, $NO_2$, ozone and $PM_{2.5}$ concentrations with the proxy-based and unit-based inventories, and the differences between the two simulations. For $SO_2$, $NO_2$ and $PM_{2.5}$, the concentrations in the urban area is generally higher with proxy-based inventory than that with

10 unit-based inventory, especially in winter. In January, large difference of concentrations of simulations with two inventories are found in urban Tianjin, Tangshan, Baoding and Shijiazhuang, where a large amount of industrial emissions are allocated in the proxy-based inventory due to large population density. The simulation of July follows the same pattern but the concentrations and the difference between the concentrations with two inventories are lower than those of January. In some areas where many factories

15 are located, such like the northern part of Xingtai city, the concentration with unit-based inventory is higher because of the high emission intensity. There are two reasons for the difference between results with two inventories. The first one is the spatial distribution. With detailed information of industrial sectors, more emissions are allocated to certain locations in suburban areas in unit-based emission inventory. The other reason is vertical distribution. Plume rise is calculated in the simulation with unit-

20 based inventory, which causes the difference of emissions in vertical layers. The higher the pollutants are emitted, the lower the ground concentration becomes. For ozone, the difference of concentration is evident but opposite to that of $PM_{2.5}$. This is because that urban centers of Beijing/Tianjin are located in the VOC-control chemical regime (Liu et al., 2010). The emissions of $NO_x$ in surface layer are less in the unit-based inventory than in the proxy-based inventory, which leads to higher ozone concentration in urban

25 area.

The spatial distribution of concentrations of these pollutants are significantly heterogeneous. For $SO_2$, $NO_2$ and $PM_{2.5}$, peak concentrations usually occur in the urban center while it's the opposite for ozone.

We apply the metric of "concentration gradient", which is defined as the ratios of urban concentrations to suburban concentrations, to quantitatively characterize the heterogeneous spatial distributions. We calculate the concentration gradients for Beijing and Tianjin (**Fig. 6**), since there are both urban and suburb observational sites in these two cities. The concentration gradient of $NO_2$ and $SO_2$ between urban and suburban areas is closer to the observations in the simulation with unit-based inventory than that with proxy-based inventory (**Fig. 6**). The simulated $O_3$ concentration gradients with unit-based, proxy-based inventories and the observation are 0.7, 0.5 and 0.9 in January and 0.9, 0.8 and 1.1 in July. As stated previously, this is explained by the VOC-limited photochemical regime and lower $NO_x$ emissions in the unit-based inventory over the urban areas. As for $PM_{2.5}$, the concentration gradients for simulations with unit-based, proxy-based inventories and observations in Beijing are 1.6, 2.1 and 1.5 in January and 1.3, 1.5 and 1.3 in July. The results imply that the unit-based emission inventory better reproduces the distributions of pollutant emissions between the urban and suburban areas.

To further elucidate the reasons for the difference between the $PM_{2.5}$ concentrations with two emission inventories, we examine the simulation results of different chemical components, including sulfate ($SO_4^{2-}$), nitrate ($NO_3^-$), ammonium ($NH_4^+$), element carbon (EC) and organic carbon (OC), as shown in **Fig. 7** and **Table 2**. The concentrations of EC and OC in the simulation with unit-based inventory are generally lower than that with proxy-based inventory in both January and July, especially in urban Beijing, Baoding and Shijiazhuang. This pattern is similar to that of $PM_{2.5}$. In some cities such as Xingtai, the concentrations of EC and OC in the simulation with unit-based inventory are slightly higher than that with proxy-based inventory.

The results of secondary inorganic aerosols are quite different. From **Fig. 7** and **Table 2** we can see that in winter the concentration of nitrate in the simulation with unit-based inventory is much higher than that with proxy-based inventory while in summer the differences between the results with two inventories vary with location. According to Zhao et al. (2017b), the sensitivity of nitrate concentration to $NO_x$ concentration is mostly negative in winter, which can partly explain the higher concentration of nitrate in winter in the simulation with unit-based inventory because of lower concentration of $NO_x$. In summer, the sensitivity of nitrate to $NO_x$ is positive. Therefore, the simulated nitrate concentrations with unit-based

inventory are lower in most areas due to lower $NO_x$ concentration but higher in certain areas with higher $NO_x$ concentration. As for sulfate, the sensitivity of sulfate concentrations to $SO_2$ concentration is positive during all months (Zhao et al., 2017b), which can explain the lower sulfate concentrations in most areas in the simulation with unit-based inventory as compared to that with proxy-based inventory. The

5    differences of the concentration of sulfate is similar to that of $SO_2$, which is shown in **Fig. 5**. Taking all chemical components into account, the primary components account for most of the differences in $PM_{2.5}$ concentrations between the simulations with two inventories. In contrast, however, the complex responses of various secondary components often counteract each other (especially in January), leading to an overall smaller contribution of secondary components to the $PM_{2.5}$ concentration differences.

10   **4 Conclusion**

In this study, we developed a high-resolution emission inventory of major pollutants for BTH region for year 2014 with unit-based emissions from industrial sectors. The emissions of $SO_2$, $NO_x$, $PM_{10}$, $PM_{2.5}$, BC, OC and NMVOCs from industrial sectors are 869 kt, 1164 kt, 910 kt, 622 kt, 71 kt, 63 kt and 1390 kt respectively, accounting for 61%, 55%, 62%, 56%, 58%, 22% and 36% of the total emissions.

15   The emissions in unit-based emission inventory are lower than that in the proxy-based emission inventory in most urban centers of the BTH region because of the concentrated emissions in point sources. The application of the unit-based emission inventory improves model-observation agreement for most pollutants. For $SO_2$, $NO_2$ and $PM_{2.5}$, the concentrations in the urban area decrease significantly and become closer to the observations mostly due to the decrease of urban emissions. For ozone, the

20   concentrations in the urban area increase slightly and also show better agreement with observations mainly due to the more reasonable allocation of $NO_x$ emissions. The improvement is particularly significant for the urban-suburban concentration gradients. For $PM_{2.5}$, the concentration gradients for the simulations with unit-based, proxy-based inventories and observations in Beijing are 1.6, 2.1 and 1.5 in January and 1.3, 1.5 and 1.3 in July. For ozone, the corresponding values are 0.7, 0.5 and 0.9 in January

and 0.9, 0.8 and 1.1 in July, implying that the unit-based emission inventory better reproduces the distributions of pollutant emissions between the urban and suburban areas.

The unit-based industrial emission inventory enables more accurate source apportionment and more reliable research on air pollution formation mechanism, and therefore contributes to the development of

5 more precisely targeted control policies. To further improve the emission inventory, it is necessary to improve the spatial allocation of emissions from non-industrial sectors, such as the residential and commercial sectors. Our previous study provides an example to develop a village-based residential emission inventory in rural Beijing (Cai et al., 2018). Such studies on high-resolution emission inventories, for both industrial and nonindustrial sources, are highly needed and should be extended to other provinces

10 and/or regions as well.

## Acknowledgements

This research has been supported by the National Natural Science Foundation of China (21625701) and the Ministry of Environmental Protection of China (DQGG0301). The simulations were completed on the "Explorer 100" cluster system of Tsinghua National Laboratory for Information Science and

15 Technology.

## References

Beijing Municipal Bureau of Statistics: Beijing Statistical Yearbook 2014, China Statistics Press, Beijing, 2015.

Boylan, J. W., and Russell, A. G.: PM and light extinction model performance metrics, goals, and criteria
20     for three-dimensional air quality models, Atmos Environ, 40, 4946-4959, 10.1016/j.atmonsenv.2005.09.087, 2006.

Cai, S., Li, Q., Wang, S., Chen, J., Ding, D., Zhao, B., Yang, D., and Hao, J.: Pollutant emissions from residential combustion and reduction strategies estimated via a village-based emission inventory in Beijing, Environmental pollution (Barking, Essex : 1987), 238, 230-237,
25     10.1016/j.envpol.2018.03.036, 2018.

Chen, L., Sun, Y., Wu, X., Zhang, Y., Zheng, C., Gao, X., and Cen, K.: Unit-based emission inventory and uncertainty assessment of coal-fired power plants, Atmos Environ, 99, 527-535, 10.1016/j.atmosenv.2014.10.023, 2014.

China Electricity Council: Annual Development Report for China Electric Power Industry 2014, China Statistics Press, Beijing, 2015.

Atmospheric Pollution Prevention and Control Action Plan: http://www.gov.cn/zwgk/2013-09/12/content_2486773.htm, 2013.

5  EPA, U.: Guidance on the Use of Models and Other Analyses for Demonstrating Attainment of Air Quality Goals for Ozone, PM2.5, and Regional Haze, 2007.

Fu, X., Wang, S. X., Zhao, B., Xing, J., Cheng, Z., Liu, H., and Hao, J. M.: Emission inventory of primary pollutants and chemical speciation in 2010 for the Yangtze River Delta region, China, Atmos Environ, 70, 39-50, 10.1016/j.atmosenv.2012.12.034, 2013.

10  Geng, G., Zhang, Q., Martin, R. V., Lin, J., Huo, H., Zheng, B., Wang, S., and He, K.: Impact of spatial proxies on the representation of bottom-up emission inventories: A satellite-based analysis, Atmos Chem Phys, 17, 4131-4145, 10.5194/acp-17-4131-2017, 2017.

Hebei Municipal Bureau of Statistics: Hebei Statistical Yearbook 2014, China Statistics Press, Hebei, 2015.

15  Lei, Y., Zhang, Q., Nielsen, C., and He, K.: An inventory of primary air pollutants and CO2 emissions from cement production in China, 1990-2020, Atmos Environ, 45, 147-154, 10.1016/j.atmosenv.2010.09.034, 2011.

Li, M., Zhang, Q., Kurokawa, J., Woo, J. H., He, K. B., Lu, Z. F., Ohara, T., Song, Y., Streets, D. G., Carmichael, G. R., Cheng, Y. F., Hong, C. P., Huo, H., Jiang, X. J., Kang, S. C., Liu, F., Su, H., and

20  Zheng, B.: MIX: a mosaic Asian anthropogenic emission inventory under the international collaboration framework of the MICS-Asia and HTAP, Atmos Chem Phys, 17, 935-963, 10.5194/acp-17-935-2017, 2017.

Lim, T. J., Lim, Y., and Liu, E. H.: Evaluation of ease of intubation with the GlideScope or Macintosh laryngoscope by anaesthetists in simulated easy and difficult laryngoscopy, Anaesthesia, 60, 180-

25  183, 10.1111/j.1365-2044.2004.04038.x, 2005.

Liu, X. H., Zhang, Y., Xing, J., Zhang, Q. A., Wang, K., Streets, D. G., Jang, C., Wang, W. X., and Hao, J. M.: Understanding of regional air pollution over China using CMAQ, part II. Process analysis and sensitivity of ozone and particulate matter to precursor emissions, Atmos Environ, 44, 3719-3727, 10.1016/j.atmosenv.2010.03.036, 2010.

30  National Bureau of Statistics (NBS): China Steel Yearbook 2011, China Statistics Press, Beijing, 2012.

National Bureau of Statistics (NBS): China Electric Power Yearbook 2014, China Statistics Press, Beijing, 2015a.

National Bureau of Statistics (NBS): China Energy Statistical Yearbook 2014, China Statistics Press, Beijing, 2015b.

35  National Bureau of Statistics (NBS): China Industrial Economic Statistical Yearbook 2014, China Statistics Press, Beijing, 2015c.

National Bureau of Statistics (NBS): China Regional Economic Statistical Yearbook 2014, China Statistics Press, Beijing, 2015d.

National Bureau of Statistics (NBS): China Rural Statistical Yearbook 2014, China Statistics Press,

40  Beijing, 2015e.

National Bureau of Statistics (NBS): China Statistical Yearbook 2014, China Statistics Press, Beijing, 2015f.

National Bureau of Statistics (NBS): China Urban Construction Statistical Yearbook 2014, China Statistics Press, Beijing, 2015g.

5  National Bureau of Statistics (NBS): China Environmental Statistical Yearbook 2014, China Statistics Press, Beijing, 2015h.

National Bureau of Statistics (NBS): China Agriculture Yearbook 2014, China Statistics Press, Beijing, 2015i.

National Bureau of Statistics (NBS): China Chemical Industry yearbook 2014, China Statistics Press,
10  Beijing, 2015j.

Oda, T., and Maksyutov, S.: A very high-resolution (1 km×1 km) global fossil fuel $CO_2$ emission inventory derived using a point source database and satellite observations of nighttime lights, Atmos Chem Phys, 11, 543-556, 10.5194/acp-11-543-2011, 2011.

Ohara, T., Akimoto, H., Kurokawa, J., Horii, N., Yamaji, K., Yan, X., and Hayasaka, T.: An Asian
15  emission inventory of anthropogenic emission sources for the period 1980-2020, Atmos Chem Phys, 7, 4419-4444, 10.5194/acp-7-4419-2007, 2007.

Qi, J., Zheng, B., Li, M., Yu, F., Chen, C., Liu, F., Zhou, X., Yuan, J., Zhang, Q., and He, K.: A high-resolution air pollutants emission inventory in 2013 for the Beijing-Tianjin-Hebei region, China, Atmos Environ, 170, 156-168, 10.1016/j.atmosenv.2017.09.039, 2017.

20  Stohl, A., Aamaas, B., Amann, M., Baker, L. H., Bellouin, N., Berntsen, T. K., Boucher, O., Cherian, R., Collins, W., Daskalakis, N., Dusinska, M., Eckhardt, S., Fuglestvedt, J. S., Harju, M., Heyes, C., Hodnebrog, O., Hao, J., Im, U., Kanakidou, M., Klimont, Z., Kupiainen, K., Law, K. S., Lund, M. T., Maas, R., MacIntosh, C. R., Myhre, G., Myriokefalitakis, S., Olivie, D., Quaas, J., Quennehen, B., Raut, J. C., Rumbold, S. T., Samset, B. H., Schulz, M., Seland, O., Shine, K. P., Skeie, R. B.,
25  Wang, S., Yttri, K. E., and Zhu, T.: Evaluating the climate and air quality impacts of short-lived pollutants, Atmos Chem Phys, 15, 10529-10566, 10.5194/acp-15-10529-2015, 2015.

Streets, D. G., Bond, T. C., Carmichael, G. R., Fernandes, S. D., Fu, Q., He, D., Klimont, Z., Nelson, S. M., Tsai, N. Y., Wang, M. Q., Woo, J. H., and Yarber, K. F.: An inventory of gaseous and primary aerosol emissions in Asia in the year 2000, J Geophys Res-Atmos, 108, 10.1029/2002jd003093,
30  2003.

Tianjin Municipal Bureau of Statistics: Tianjin Statistical Yearbook 2014, China Statistics Press, Tianjin, 2015.

Wang, K., Tian, H., Hua, S., Zhu, C., Gao, J., Xue, Y., Hao, J., Wang, Y., and Zhou, J.: A comprehensive emission inventory of multiple air pollutants from iron and steel industry in China: Temporal trends
35  and spatial variation characteristics, Sci Total Environ, 559, 7-14, 10.1016/j.scitotenv.2016.03.125, 2016.

Wang, S. X., Zhao, B., Cai, S. Y., Klimont, Z., Nielsen, C. P., Morikawa, T., Woo, J. H., Kim, Y., Fu, X., Xu, J. Y., Hao, J. M., and He, K. B.: Emission trends and mitigation options for air pollutants in East Asia, Atmos Chem Phys, 14, 6571-6603, DOI 10.5194/acp-14-6571-2014, 2014.

Wu, W., Zhao, B., Wang, S., and Hao, J.: Ozone and secondary organic aerosol formation potential from anthropogenic volatile organic compounds emissions in China, J Environ Sci (China), 53, 224-237, 10.1016/j.jes.2016.03.025, 2017.

Xue, Y., Tian, H., Yan, J., Zhou, Z., Wang, J., Nie, L., Pan, T., Zhou, J., Hua, S., Wang, Y., and Wu, X.: Temporal trends and spatial variation characteristics of primary air pollutants emissions from coal-fired industrial boilers in Beijing, China, Environ Pollut, 213, 717-726, 10.1016/j.envpol.2016.03.047, 2016.

Zhao, B., Wang, S., Dong, X., Wang, J., Duan, L., Fu, X., Hao, J., and Fu, J.: Environmental effects of the recent emission changes in China: implications for particulate matter pollution and soil acidification, Environmental Research Letters, 8, 024031, 10.1088/1748-9326/8/2/024031, 2013a.

Zhao, B., Wang, S. X., Wang, J. D., Fu, J. S., Liu, T. H., Xu, J. Y., Fu, X., and Hao, J. M.: Impact of national NOx and SO2 control policies on particulate matter pollution in China, Atmos Environ, 77, 453-463, 10.1016/j.atmosenv.2013.05.012, 2013b.

Zhao, B., Wang, S., Donahue, N. M., Jathar, S. H., Huang, X., Wu, W., Hao, J., and Robinson, A. L.: Quantifying the effect of organic aerosol aging and intermediate-volatility emissions on regional-scale aerosol pollution in China, Sci Rep, 6, 28815, 10.1038/srep28815, 2016.

Zhao, B., Wu, W., Wang, S., Xing, J., Chang, X., Liou, K.-N., Jiang, J. H., Gu, Y., Jang, C., Fu, J. S., Zhu, Y., Wang, J., Lin, Y., and Hao, J.: A modeling study of the nonlinear response of fine particles to air pollutant emissions in the Beijing-Tianjin-Hebei region, Atmos Chem Phys, 17, 12031-12050, 10.5194/acp-17-12031-2017, 2017a.

Zhao, B., Wu, W. J., Wang, S. X., Xing, J., Chang, X., Liou, K. N., Jiang, J. H., Gu, Y., Jang, C., Fu, J. S., Zhu, Y., Wang, J. D., Lin, Y., and Hao, J. M.: A modeling study of the nonlinear response of fine particles to air pollutant emissions in the Beijing-Tianjin-Hebei region, Atmos Chem Phys, 17, 12031-12050, 10.5194/acp-17-12031-2017, 2017b.

Zhao, Y., Wang, S. X., Duan, L., Lei, Y., Cao, P. F., and Hao, J. M.: Primary air pollutant emissions of coal-fired power plants in China: Current status and future prediction, Atmos Environ, 42, 8442-8452, 10.1016/j.atmosenv.2008.08.021, 2008.

Zhao, Y., Mao, P., Zhou, Y. D., Yang, Y., Zhang, J., Wang, S. K., Dong, Y. P., Xie, F. J., Yu, Y. Y., and Li, W. Q.: Improved provincial emission inventory and speciation profiles of anthropogenic non-methane volatile organic compounds: a case study for Jiangsu, China, Atmos Chem Phys, 17, 7733-7756, 10.5194/acp-17-7733-2017, 2017c.

Zheng, B., Zhang, Q., Tong, D., Chen, C., Hong, C., Li, M., Geng, G., Lei, Y., Huo, H., and He, K.: Resolution dependence of uncertainties in gridded emission inventories: a case study in Hebei, China, Atmos Chem Phys, 17, 921-933, 10.5194/acp-17-921-2017, 2017.

Zhou, Y., and Gurney, K. R.: Spatial relationships of sector-specific fossil fuel CO2emissions in the United States, Global Biogeochemical Cycles, 25, n/a-n/a, 10.1029/2010gb003822, 2011.

# Figures
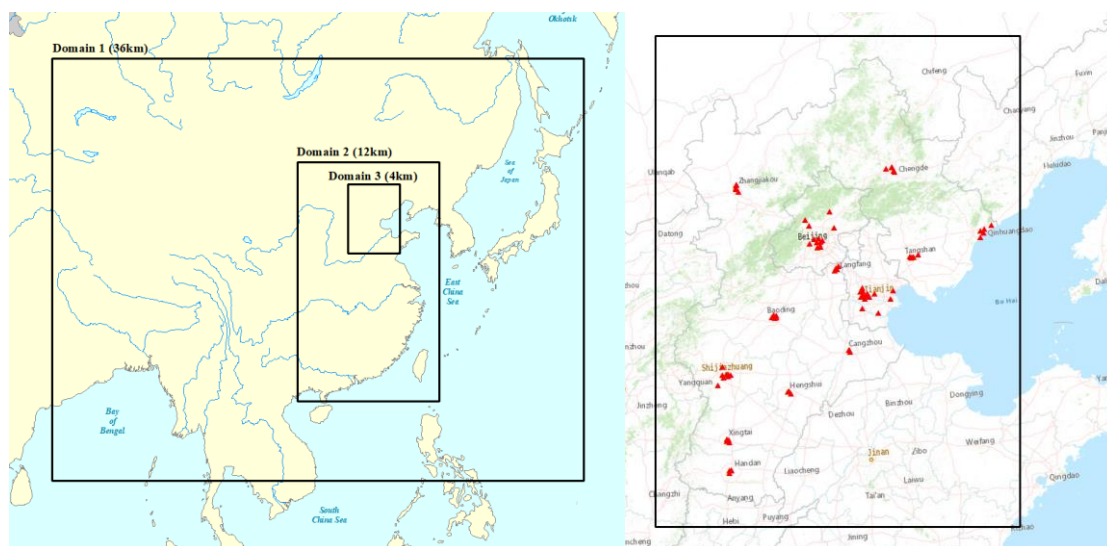
**Fig. 1 The three-nested CMAQ domain (left) and the observational sites in Beijing-Tianjin-Hebei region (right)**
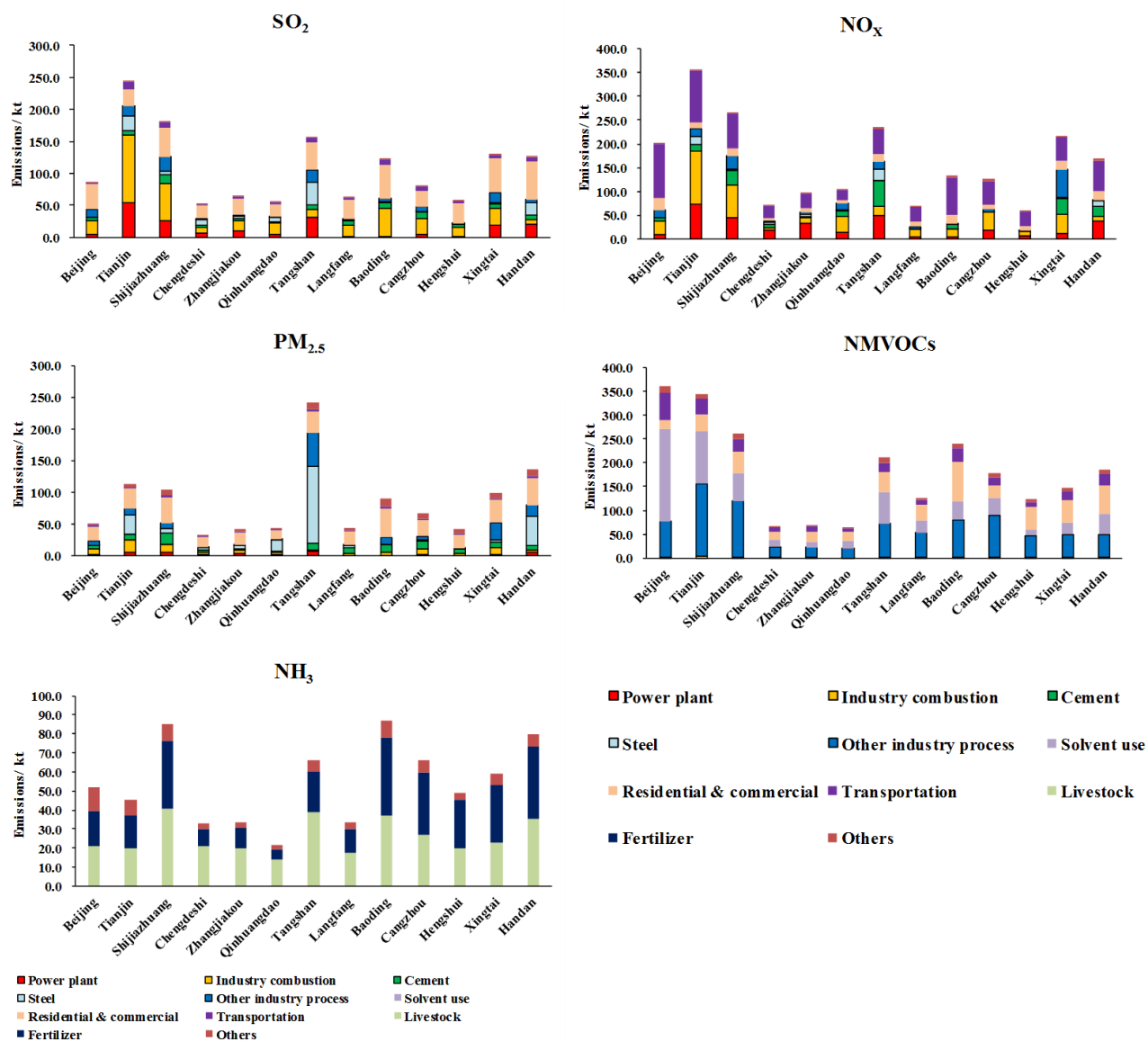
**Fig. 2 Sectoral contributions to emissions in BTH region in 2014**
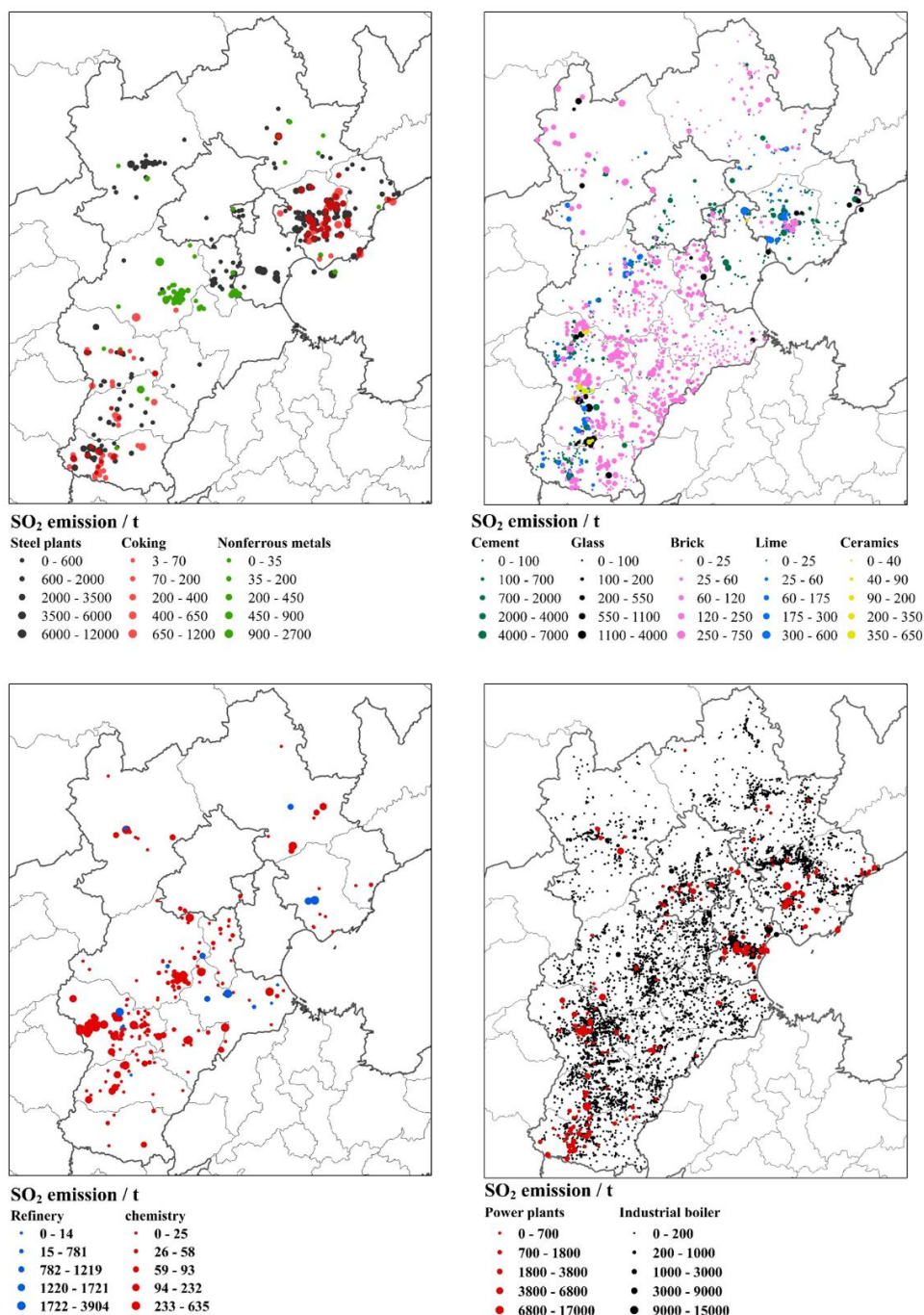
**Fig. 3 Locations and emissions of industrial sources in the BTH region. The industrial plants are divided into four groups to display more clearly.**
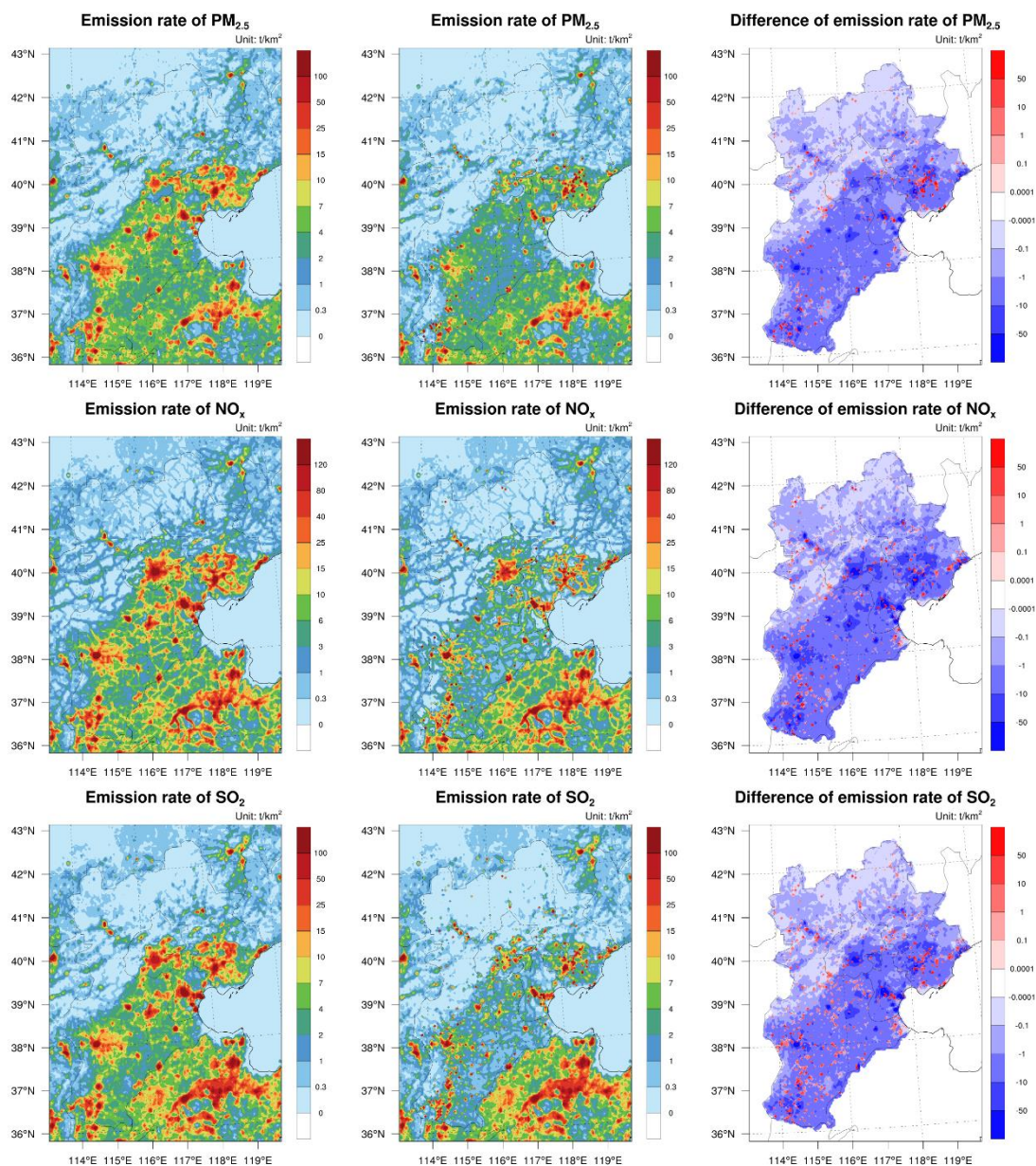
**Fig. 4 Emission rate of PM₂.₅, NOₓ and SO₂ emissions of the proxy-based (left column) and unit-based (middle column) inventories and their differences (unit-based minus proxy-based, right column). Note that the emissions are the same in provinces other than Beijing, Tianjin, and Hebei.**
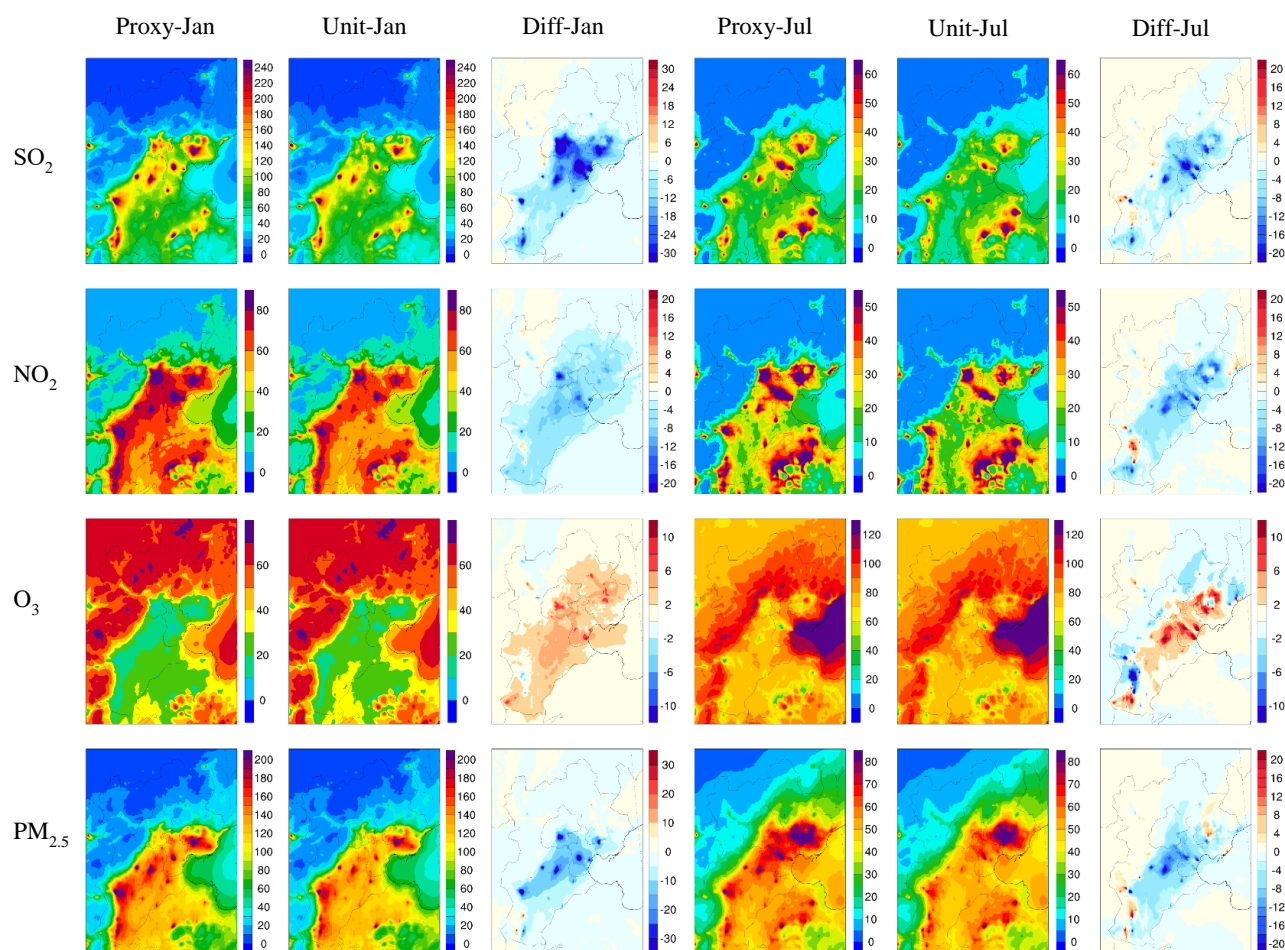
**Fig. 5 Spatial distribution of the monthly (January and July) mean concentrations of SO₂, NO₂, ozone and PM₂.₅ with the proxy-based, unit-based inventories, and the differences between these two simulations (unit-based minus proxy-based). The units are µg/$m^3$ for all panels.**
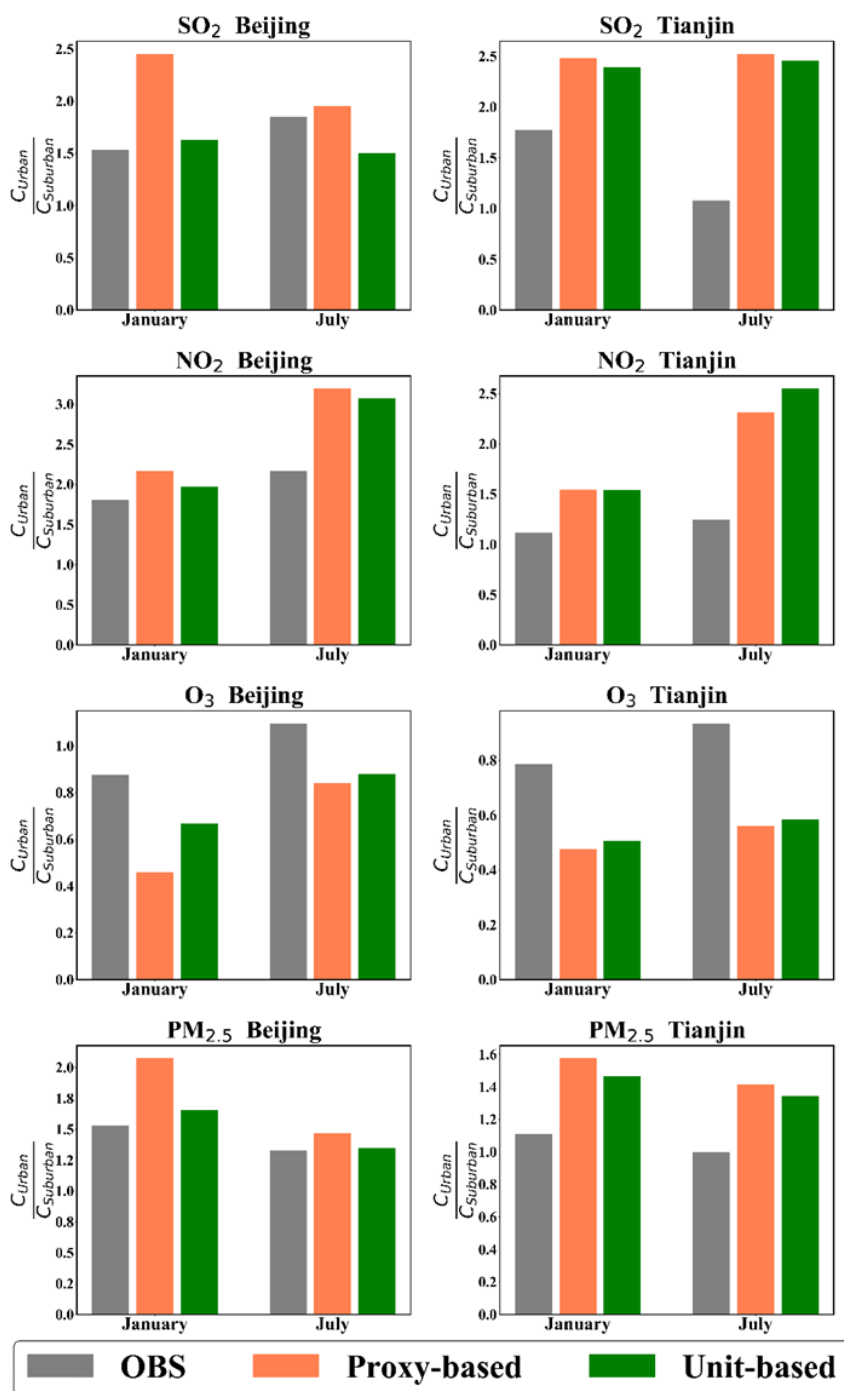
**Fig. 6 Observed and simulated concentration gradients of NO₂, PM₂.₅, ozone and SO₂ with the unit-based and proxy-based inventories in Beijing (left) and Tianjin (right)**
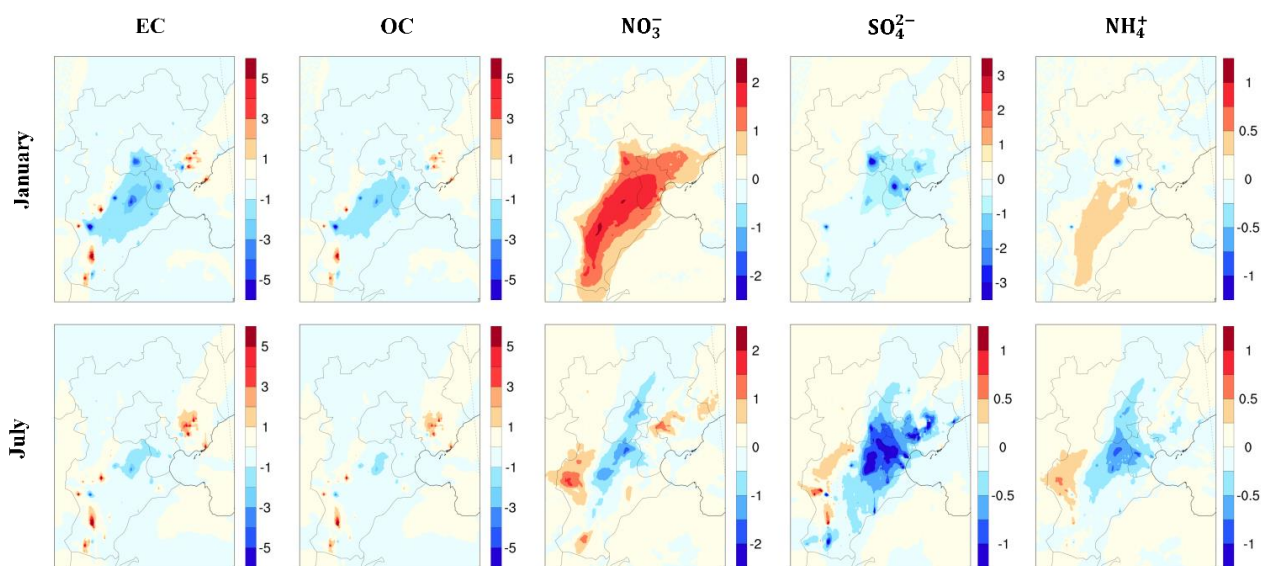
**Fig. 7 The differences (unit: μg/$m^3$) in the simulation results of the components of PM₂.₅ between the results with two inventories (unit-based minus proxy-based).**

**Table 1. The statistics for model performance of PM₂.₅, NO₂, SO₂ and ozone in January and July of 2014 with proxy-based and unit-based inventories**

| Month | Species | Emission | SIM ( $\mu g/m^3$ ) | OBS ( $\mu g/m^3$ ) | NME | NMB | MFB | MFE |
|-------|---------|----------|-----|-----|-----|-----|-----|-----|
| Jan | SO₂ | Proxy-based | 251.9 | 112.3 | 131% | 124% | 51% | 57% |
| | | Unit-based | 207.8 | 112.3 | 93% | 85% | 35% | 42% |
| | NO₂ | Proxy-based | 88.0 | 72.0 | 30% | 22% | 14% | 19% |
| | | Unit-based | 77.9 | 72.0 | 23% | 8% | 5% | 16% |
| | O₃ | Proxy-based | 16.8 | 21.4 | 36% | -21% | -19% | 27% |
| | | Unit-based | 20.2 | 21.4 | 33% | -6% | -6% | 22% |
| | PM₂.₅ | Proxy-based | 176.3 | 141.1 | 39% | 25% | 12% | 22% |
| | | Unit-based | 151.5 | 141.1 | 31% | 7% | 2% | 20% |
| Jul | SO₂ | Proxy-based | 58.4 | 26.4 | 140% | 121% | 54% | 63% |
| | | Unit-based | 42.7 | 26.4 | 86% | 62% | 34% | 47% |
| | NO₂ | Proxy-based | 61.5 | 35.9 | 80% | 72% | 33% | 40% |
| | | Unit-based | 52.1 | 35.9 | 62% | 45% | 20% | 34% |
| | O₃ | Proxy-based | 64.0 | 66.8 | 96% | -4% | -26% | 26% |
| | | Unit-based | 69.0 | 66.8 | 90% | 3% | -21% | 22% |
| | PM₂.₅ | Proxy-based | 71.2 | 85.5 | 26% | -17% | -12% | 19% |
| | | Unit-based | 60.1 | 85.5 | 34% | -30% | -21% | 25% |
| Annual average | SO₂ | Proxy-based | 155.2 | 69.4 | 133% | 124% | 53% | 60% |
| | | Unit-based | 125.2 | 69.4 | 92% | 81% | 35% | 45% |
| | NO₂ | Proxy-based | 74.7 | 53.9 | 47% | 39% | 23% | 30% |
| | | Unit-based | 65.0 | 53.9 | 36% | 21% | 13% | 25% |
| | O₃ | Proxy-based | 40.4 | 44.1 | 82% | -8% | -22% | 27% |
| | | Unit-based | 44.6 | 44.1 | 76% | 1% | -14% | 22% |
| | PM₂.₅ | Proxy-based | 123.8 | 113.3 | 34% | 9% | 0% | 21% |
| | | Unit-based | 105.8 | 113.3 | 32% | -7% | -10% | 23% |

**Table 2. The mean concentrations (unit: μg/$m^3$) of the components of PM2.5 with proxy-based and unit-based inventories and their differences**

| Month | Emission | EC | OC | $NO_3^-$ | $SO_4^{2-}$ | $NH_4^+$ |
|-------|----------|------|------|------|------|------|
| | Proxy-based | 41.2 | 49.7 | 11.8 | 11.7 | 7.8 |
| Jan | Unit-based | 38.5 | 48.0 | 13.0 | 10.2 | 7.6 |
| | difference | -7% | -4% | 10% | -12% | -2% |
| | Proxy-based | 8.3 | 9.3 | 11.9 | 10.2 | 7.3 |
| Jul | Unit-based | 7.1 | 8.4 | 11.8 | 9.3 | 6.9 |
| | difference | -15% | -9% | 0% | -9% | -5% |